Pharmacological inhibition of MEK1/2 signaling disrupts bile acid metabolism through loss of Shp and enhanced Cyp7a1 expression

Verzijl, Cristy R C; van de Peppel, Ivo P; Eilers, Roos E; Bloks, Vincent W; Wolters, Justina C; Koehorst, Martijn; Kloosterhuis, Niels J; Havinga, Rick; Jalving, Mathilde; Struik, Dicky

Published in:
Biomedicine & pharmacotherapy = Biomedecine & pharmacotherapie

DOI:
10.1016/j.biopha.2023.114270

Publication date:
2023

Biomedicine & Pharmacotherapy 159 (2023) 114270

Contents lists available at ScienceDirect

Biomedicine & Pharmacotherapy

journal homepage: www.elsevier.com/locate/biopha

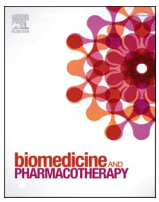

Pharmacological inhibition of MEK1/2 signaling disrupts bile acid metabolism through loss of *Shp* and enhanced *Cyp7a1* expression

Cristy R.C. Verzijl [a], Ivo P. van de Peppel [a], Roos E. Eilers [a], Vincent W. Bloks [a], Justina C. Wolters [a], Martijn Koehorst [b], Niels J. Kloosterhuis [a], Rick Havinga [a], Mathilde Jalving [c], Dicky Struik [a], Johan W. Jonker [a,*]

[a] Department of Pediatrics, University of Groningen, University Medical Center Groningen, Groningen, The Netherlands
[b] Department of Laboratory Medicine, University of Groningen, University Medical Center Groningen, 9713 Groningen, GZ, The Netherlands
[c] Department of Medical Oncology, University of Groningen, University Medical Center Groningen, Groningen, The Netherlands

ARTICLE INFO

Keywords:
Bile acid metabolism
Liver toxicity
MEK inhibition
Cancer treatment
RAS-MAPK signaling

ABSTRACT

The RAS-MAPK signaling pathway is one of the most frequently dysregulated pathways in human cancer. Small molecule inhibitors directed against this pathway have clinical activity in patients with various cancer types and can improve patient outcomes. However, the use of these drugs is associated with adverse effects, which can result in dose reduction or treatment interruption. A better molecular understanding of on-target, off-tumor effects may improve toxicity management. In the present study, we aimed to identify early initiating biological changes in the liver upon pharmacological inhibition of the RAS-MAPK signaling pathway. To this end, we tested the effect of MEK inhibitor PD0325901 using mice and human hepatocyte cell lines. Male C57BL/6 mice were treated with either vehicle or PD0325901 for six days, followed by transcriptome analysis of the liver and phenotypic characterization. Pharmacological MEK inhibition altered the expression of 423 genes, of which 78 were upregulated and 345 were downregulated. We identified *Shp*, a transcriptional repressor, and *Cyp7a1*, the rate-limiting enzyme in converting cholesterol to bile acids, as the top differentially expressed genes. PD0325901 treatment also affected other genes involved in bile acid regulation, which was associated with changes in the composition of plasma bile acids and composition and total levels of fecal bile acids and elevated predictive biomarkers of early liver toxicity. In conclusion, short-term pharmacological MEK inhibition results in profound changes in bile acid metabolism, which may explain some of the clinical adverse effects of pharmacological inhibition of the RAS-MAPK pathway, including gastrointestinal complications and hepatotoxicity.

1. Introduction

Receptor tyrosine kinases (RTK) are membrane-spanning cell surface receptors involved in a broad range of basal cellular processes, including proliferation, differentiation, metabolism, and survival. Ligand binding causes receptor dimerization, leading to autophosphorylation and subsequent activation of downstream canonical signaling pathways [1,2]. Receptor-specific ligands include growth factors, such as fibroblast growth factors (FGFs), epidermal growth factor (EGF), platelet-derived growth factor (PDGF), insulin, and insulin-like growth factor (IGF).

Abbreviations: MEK, Mitogen-activated protein kinase kinase; ERK, extracellular signal-regulated protein kinase; RTK, Receptor tyrosine kinase; FGF, fibroblast growth factor; EGF, epidermal growth factor; PDGF, platelet-derived growth factor; IGF, insulin-like growth factor; FDA, Food and Drug Administration; NSCLC, non-small cell lung cancer; ATC, anaplastic thyroid cancer; NF1, neurofibromatosis type 1; CYP7A1, cytochrome P450, family 7, subfamily a, polypeptide 1; SHP/NR0B2, small heterodimer partner; CYP8B1, cytochrome P450 family 8 subfamily B member 1; CYP27A1, cytochrome P450 family 27 subfamily A member 1; CYP7B1, cytochrome P450 family 7 subfamily B member 1; NTCP/SLC10A1, sodium/bile acid cotransporter; OATP1/SLCO1A1, organic anion transporting polypeptide 1; FXR/NR1H4, farnesoid x receptor; BSEP/ABCB11, bile acid export pump; ASBT/SLC10A2, apical sodium dependent bile acid transporter; OSTβ/SLC51B, organic solute transporter beta; IBABP/FABP6, ileal bile acid-binding protein; CA, cholic acid; DCA, deoxycholic acid; MCA, muricholic acid; UDCA, ursodeoxycholic acid; ALT, alanine transaminase; AST, aspartate transaminase; CRAT, carnintine-O-acetyltransferase; TKFC, triokinase/FMN cyclase; CAR3, carbonic anhydrase 3; PD-1, programmed death 1.

* Correspondence to: University Medical Center Groningen, Laboratory of Pediatrics, Groningen, the Netherlands.
E-mail address: j.w.jonker@umcg.nl (J.W. Jonker).

https://doi.org/10.1016/j.biopha.2023.114270
Received 2 December 2022; Received in revised form 6 January 2023; Accepted 16 January 2023
Available online 19 January 2023

The RAS-MAPK pathway is one of the canonical pathways downstream of RTKs that is tightly regulated to ensure fine-tuning of gene expression programs and translational events. Activation of the RTK results in the activation of RAS and the recruitment of RAF. Activated RAF mediates the phosphorylation of mitogen-activated protein kinase kinases 1 and − 2 (MEK1 and 2), which in turn phosphorylate extracellular signal-regulated protein kinases 1 and − 2 (ERK1 and ERK2) [3]. ERK can then translocate to the nucleus to phosphorylate substrates, e.g., transcription factors, or stay in the cytoplasm to phosphorylate other proteins and kinases [4].

Components of the RAS-MAPK pathway are mutated or aberrantly expressed in more than 40 % of human cancers [5]. Oncogenic activation of this pathway is mainly driven by mutationally activated Ras or B-Raf. Irregularities can also occur upstream, at the level of the RTK, leading to uncontrolled tumor cell proliferation and cell survival. B-Raf inhibitors have a limited response duration because of ERK reactivation, especially in tumors harboring BRAF V600E mutations [6,7]. To overcome this limitation, selective MEK1/2 inhibitors have been developed and evaluated in clinical studies to use as single agents or in combination regimens. The MEK1/2 inhibitor Trametinib was the first to be approved by the Food and Drug Administration (FDA) for the treatment of B-Raf mutated melanoma, non-small cell lung cancer (NSCLC), and anaplastic thyroid cancer (ATC), in combination with BRAF inhibitors (reviewed by Subbiah et al., 2020). Currently, several MEK1/2 inhibitors, including trametinib, binimetinib, and cobimetinib, are FDA-approved for combination therapies or as single agents for various cancers. Selumetinib has recently been approved for the treatment of pediatric patients with neurofibromatosis type 1 (NF1) [8].

Because the RAS-MAPK signaling pathway plays a role in a broad range of biological processes, pharmacological inhibition of this pathway is also associated with adverse events. Common side effects, which are drug- and target-dependent, include rash, diarrhea, vomiting, and abdominal pain, cardiac toxicity, retinopathy, and liver toxicity [8–10]. These side effects may result in dose reduction, interruption, or discontinuation of treatment. However, surprisingly little is known about the mechanisms underlying these on-target, off-tumor effects [9,11–13]. Improved molecular understanding can improve toxicity management and thus increase the number of patients that can be safely treated with these drugs. Because the liver plays a major role in drug metabolism, we aimed to delineate the molecular origins of the toxicity in this organ upon therapeutic inhibition of MEK1/2, a central hub in the RAS-MAPK pathway [14]. We evaluated PD0325901 (mirdametinib), a second-generation MEK inhibitor currently in phase 2 clinical trials as a monotherapy or combination therapy for different types of cancer, including NF1 and metastatic solid tumors [15–17]. For the present study, we focused on the short-term effects of PD0325901 to identify the initiating biological alterations upon MEK inhibition preceding potential clinical adverse effects.

2. Methods

2.1. Animals

This study was performed in male C57BL/6 J mice fed a standard chow diet (RM1; SDS Diets, Woerden, The Netherlands). Mice were housed in a light- and temperature-controlled facility with a 12-h light/dark cycle at 21 °C with free access to water and a chow diet. Animal experiments were performed with the approval of the National Ethics Committee for Animal Experiments of The Netherlands, following relevant guidelines and regulations (including laboratory and biosafety regulations).

2.2. Animal experiments

Male C57BL/6 J mice at ten weeks of age were individually housed. Body weight, food intake, and random glucose levels were measured daily using a glucometer (Accu-Check Performa, Roche). For PD0325901 (Selleckchem, #S1036) treatment, mice received a dose of 10 mg/kg/day PD0325901 in 1 % DMSO, 0.5 % cellulose, and 2 % Tween 80 via oral gavage for six consecutive days. At the end of the treatment period, mice were anesthetized by intraperitoneal injection of hypnorm (1 mL/kg fentanyl-fluanisone) and diazepam (10 mg/kg) followed by gall-bladder cannulation as described previously [18]. Bile was collected for 30 min after which mice were terminated by cardiac puncture under isoflurane anesthesia followed by cervical dislocation. The liver and different sections of the intestine (jejunum, duodenum, and ileum) were collected and snap-frozen in liquid nitrogen and stored at − 80°C until further analysis. Blood was drawn by cardiac puncture and plasma was collected after centrifugation at 1000 x *g* for 10 min at 4 °C.

2.3. Quantitative real-time PCR

Frozen liver tissue was homogenized in QIAzol Lysis Reagent (Qiagen), and total RNA was isolated using the RNAeasy mini kit (Qiagen, #74104). Two μg of total RNA was used for cDNA synthesis according to the manufacturer protocol (Invitrogen, #28025013). Twenty ng of cDNA was used for quantitative real-time PCR (qRT-PCR) analysis using SYBR Green Master Mix (Roche) and qRT-PCR primers. QRT-PCR data were analyzed using QuantStudio™ Real-Time PCR software, and expression was normalized to housekeeping genes and expressed as fold change compared to vehicle-treated mice.

2.4. RNA sequencing

For RNA sequencing analysis total RNA was first analyzed for quality using a nanodrop. Library preparation, sequencing, and basic analysis were done by Novogene Co. Ltd. Europe. Differential expression analysis between two groups (n = 6 per group) was performed using the DESeq2 R package. The resulting P-values were adjusted using the False Discovery Rate (FDR). Heatmaps were constructed based on the z-score calculated from the FPKM scores. Venny 2.1 [19] and Clustvis were used for further data analysis.

2.5. Immunoblotting

Tissue and cell homogenates were obtained using NP40 buffer (0.1 % Nonidet P-40 [NP-40], 0.4 M NaCl, 10 mM Tris-HCl [pH 8.0], 1 mM EDTA) supplemented with protease and phosphatase inhibitors (Roche). Protein concentration was determined using the Bradford assay (Bio-Rad). A total of 15–20 μg of protein per sample was separated using SDS-PAGE and transferred to PVDF Transfer Membrane (Amersham™ Hybond™ –P, GE Healthcare; RPN303F). Membranes were blocked in 5 % BSA in Tris-buffered saline with 0.01 % Tween 20 (Millipore Sigma) and incubated with the indicated antibodies. Proteins were visualized using a ChemiDoc XRS + System using Image Lab software version 5.2.1 (Bio-Rad).

2.6. Antibodies

The following primary antibodies were used for Western blotting: rabbit-anti-p44/42 MAPK (Cell Signaling, #4695), rabbit-anti-phospho-p44/42 MAPK (Cell Signaling, #4370), rabbit-anti-Hsp90 (Cell Signaling, #4874), rabbit-anti-MEK1/2 (Cell Signaling, #9122), rabbit-anti-phosho-MEK1/2 (Ser217/221) (Cell Signaling, #9154) and rabbit-anti-EGR1 (Cell Signaling, #4153). The secondary antibody used for western blotting was goat-anti-rabbit IgG-HRP conjugate (Bio-rad, #1706515).

2.7. Targeted proteomics

To quantify proteins involved in hepatic bile acid metabolism,

targeted proteomics was performed using isotopically labeled peptide standards (containing ^{13}C-labeled lysines or arginines) derived from synthetic protein concatamers (QconCAT) (PolyQuant GmbH, Germany), as described previously [20]. Peptide sequences that were used for the peptide quantification are listed in Supplemental Table 9 (Table S9). For the detection of the low abundant protein CYP7A1, protein samples were rerun on an SDS-PAGE gel for approximately 20 min followed by excision and in-gel digestion of the band corresponding to the size between 35 kDa and just above 70 kDa.

2.8. Bile acid analysis

Bile acids in plasma and bile were analyzed by ultra high-performance liquid chromatography-tandem mass spectrometry (HPLC-MS/MS), and fecal bile acids were analyzed by gas-liquid chromatography, as described previously [21].

2.9. Cell culture

For *in vitro* studies, human hepatocyte cell lines HepG2 (ATCC), Hep3B (ATCC), and immortalized human hepatocytes (IHH) [22], and the human colorectal cell line Caco-2 (ATCC) were used. HepG2, Hep3B, and Caco-2 cells were maintained in high glucose Dulbecco's Modified Eagle Medium (DMEM) + GlutaMAX supplemented with 10 % heat-inactivated fetal calf serum (FCS), 100 U/mL penicillin, and 100 μg/mL streptomycin. IHH cells were maintained in Williams E medium containing 11 mM glucose, supplemented with 10 % heat-inactivated fetal calf serum (FCS), 100 U/mL penicillin and 100 μg/mL streptomycin, 1 pM human insulin, and 1 μM dexamethasone. Differentiation of Caco-2 cells into intestinal-like enterocytes was achieved by maintaining the cells at 100 % confluence for three weeks.

2.10. Cell experiments

For inhibitor studies in cell lines, cells were starved for 4 h in Opti-MEM followed by inhibitor treatments for indicated time points at indicated doses. For experiments with BRAF inhibitors vemurafenib (Selleckchem, #S1267) and dabrafenib (Selleckchem, #S2807) and MEK inhibitors selumetinib (Selleckchem, #S1008), trametinib and PD0325901 (Selleckchem, #S1036), cells were starved for 4 h in Opti-MEM followed by 100 nM inhibitor treatment for 6 h after which cells were collected for immunoblotting and qPCR. For experiments using FGFR inhibitors erdafitinib (Selleckchem, #S8401), infigratinib (Selleckchem, #S2183), and pemigatinib (Selleckchem, #S0088), mTOR inhibitor everolimus (Selleckchem, #S1120), EGFR inhibitors gefitinib (Axon Medchem, #1393), and osimertinib (Axon Medchem, #2342), VEGFR inhibitor cediranib (Axon Medchem, #1461), PDGFR inhibitor imatinib (Axon Medchem, #1394), IR inhibitors linsitinib (Axon Medchem, #1702) and ceritinib (Axon Medchem, #2224) and combination inhibitors sorafenib (Axon Medchem, #3351) (inhibits VEGFR, PDGFR, and RAF) and sunitinib (Axon Medchem, #1398) (inhibits PDGFR and VEGFR), cells were starved for 4 h in Opti-MEM followed by 1 μM inhibitor treatment for 6 h after which cells were collected for immunoblotting and qPCR.

2.11. Statistics

Statistical analysis was performed using GraphPad Prism 9.0 software package (GraphPad Software, San Diego, Ca, USA). Significance was determined using an unpaired t-test when comparing two groups after testing for normality using QQplot. All values are given as means ± SEM or as boxplots with mean ± min/max. A P-value of less than 0.05 was considered statistically significant. Significance was indicated as *P < 0.05, * *P < 0.01, * **P < 0.001, * ** *P < 0.0001.

3. Results

3.1. Effect of MEK inhibition on the hepatic transcriptome

To investigate the effect of MEK inhibitor treatment on hepatic function, C57BL/6 J male mice were treated with PD0325901 (10 mg/kg) or vehicle via daily oral gavage for six consecutive days. Inhibition of MEK by PD0325901 was confirmed by western analysis, showing a strong decrease of phosphorylated ERK compared to total ERK in the liver (Fig. 1A, B). Next, we assessed the effects of MEK inhibition on the hepatic transcriptome. RNA sequencing revealed that 423 genes were differentially expressed (based on the adjusted P-value of 0.05 and FDR < 10 %), of which the majority (345) were downregulated while 78 genes were upregulated (Fig. 1C, D). Genes involved in the RAS-MAPK signaling pathway were mostly reduced in PD0325901-treated mice versus vehicle-treated mice (Fig. 2A). In addition to RAS-MAPK signaling, DAVID KEGG pathway analysis revealed a significant enrichment in genes involved in multiple signaling pathways, such as *Rap1*, *PI3K-Akt*, *FoxO,* and *Ras* signaling pathways (Fig. S1). Furthermore, we also observed an enrichment in genes involved in bile acid homeostasis (Fig. S1). We identified cytochrome P450, family 7, subfamily a, polypeptide 1 (*Cyp7a1*) – the rate-limiting enzyme in the first step of bile acid synthesis – as the top differentially expressed gene with a log fold change of 3.06 (fold change of 8.3) in PD0325901-treated mice versus vehicle-treated mice (adjusted P-value = 1.59E-21) (Fig. 1D).

3.2. Effect of MEK inhibition on the expression of genes regulating bile acid metabolism

Further stratification showed a bidirectional effect of PD0325901 treatment on bile acid metabolism related genes, including both up- and downregulated genes (Fig. 2B). Apart from *Cyp7a1*, other key genes involved in bile acid synthesis, including cytochrome P450 family 8 subfamily B member 1 (*Cyp8b1*), cytochrome P450 family 27 subfamily A member 1 (*Cyp27a1*), and cytochrome P450 family 7 subfamily B member 1 (*Cyp7b1*) were generally upregulated (Fig. 2B). Genes involved in bile acid uptake were also differentially expressed upon PD0325901 treatment, including upregulation of sodium/bile acid cotransporter (*Ntcp/Slc10a1),* and downregulation of organic anion transporting polypeptide 1 (*Oatp1/Slco1a1*), while genes involved in bile acid efflux were not greatly affected (Fig. 2B). Disruption of bile acid metabolism was also suggested by profound changes in bile acid regulators. We observed a downregulation of the bile acid-regulated transcriptional regulator small heterodimer partner (*Shp/Nr0b2,* log fold change = −1.92, adjusted P-value = 1.64E-7), likely explaining the upregulation of some *Shp*-regulated genes, including *Cyp7a1*, *Cyp8b1*, *Ntcp,* and transcription factor farnesoid x receptor (*Fxr/Nr1h4)* (Figs. 2B, S2A, and S2B).

3.3. Effect of MEK inhibition on proteins involved in bile acid metabolism

Next, we evaluated whether the observed changes in the expression of genes involved in bile acid metabolism also led to changes in protein levels using a targeted proteomics approach. In line with its mRNA levels, we found increased CYP7A1 protein levels (~21 %) (Fig. 3A). Protein levels of other genes involved in bile acid metabolism (CYP8B1, CYP27A1, ACOX2, AKR1D1, AMACR, BAAT, HSD17B4, MDR2, HNF4a, and CHREBP) were not affected except for sodium/bile acid cotransporter (NTCP) and the bile acid export pump (BSEP), which were significantly reduced (Fig. 3B). Because the intestine also plays a central role in bile acid homeostasis, we also measured the expression of genes involved in bile acid homeostasis in the ileum, where bile acid reabsorption mainly takes place. PD0325901 treatment significantly decreased the ileal expression of the apical sodium-dependent bile acid transporter (*Asbt/Slc10a2*), which is responsible for the majority of

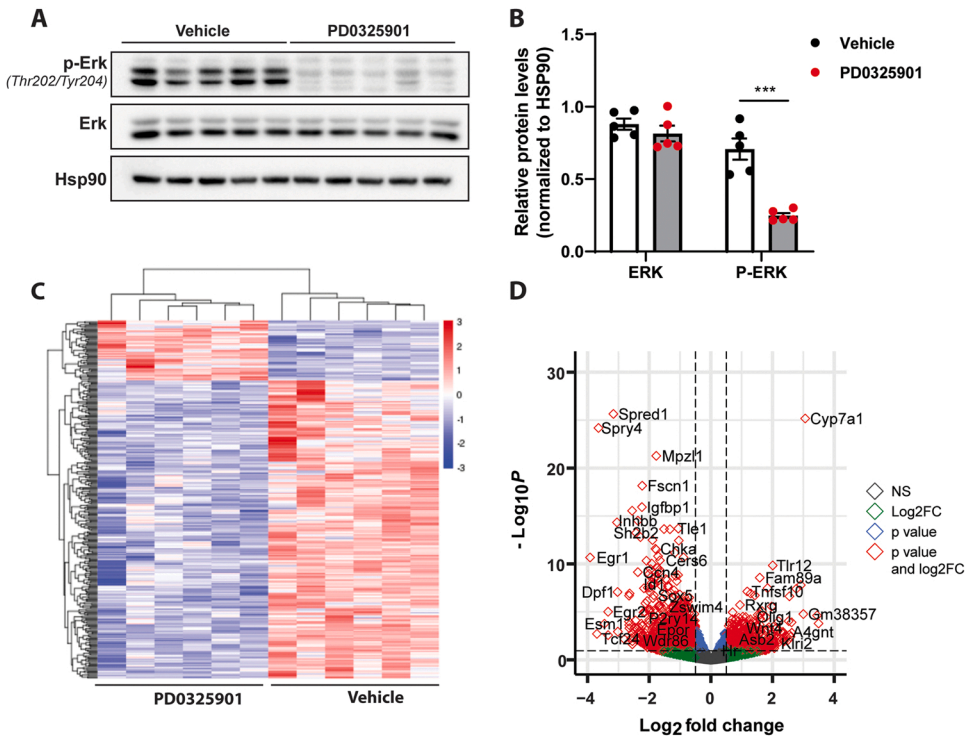

Fig. 1. Effective MEK inhibitor treatment results in global gene expression alterations. (A) Western blot shows that PD0325901 treatment results in a decrease in phosphorylated Erk (Thr202/Thr204) while total Erk remains unaltered, quantified in (B) where protein levels are normalized to Hsp90 (n = 5, same effect observed in all n = 9 mice). (C) Heatmap of differentially expressed genes in the liver between PD0325901-treated and vehicle-treated mice (n = 6, FDR 5 %). (D) Volcanoplot showing the differentially expressed genes with $\log_2$ fold change of > 0.5. Data shown as mean ± SEM with * indicating $p < 0.05$ and * ** $p < 0.001$.

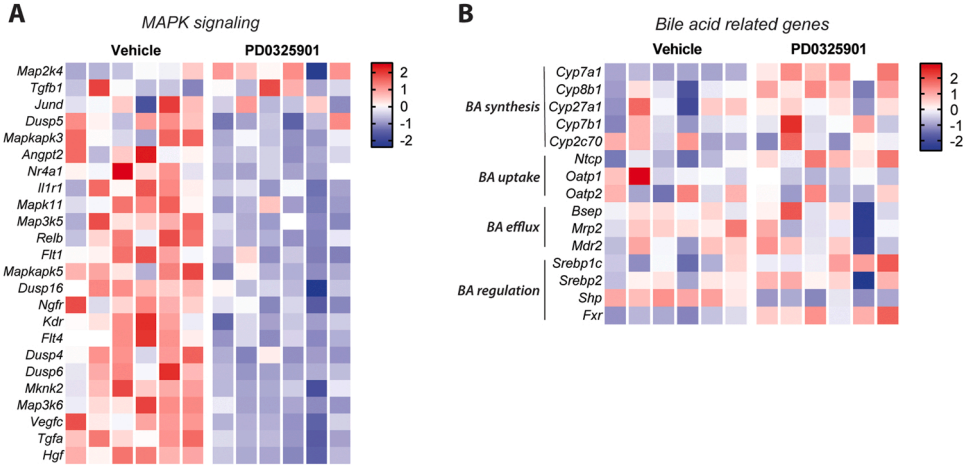

Fig. 2. PD0325901 treatment results in changes in genes involved in MAPK signaling and bile acid regulation. Heatmap presenting the z-score normalized RNA expression (FPKM values) as determined by RNA sequencing analysis of (A) MAPK signaling and (B) genes related to bile acid homeostasis (n = 6).

intestinal bile acid reabsorption as it transports conjugated bile acids [23] (Fig. 3C). PD0325901 treatment also decreased mRNA expression of the alternatively spliced form of *Asbt* (*t-Asbt*), which functions as a bile acid efflux protein, and of organic solute transporter beta (*Ostβ/Slc51b*), one of the primary bile acid efflux transporters at the basolateral side. The mRNA expression of the common ileal bile acid regulators *Shp* and ileal bile acid-binding protein (*Ibabp/Fabp6*), remained unchanged after PD0325901 treatment (Fig. 3C).

3.4. Effect of MEK inhibition on bile acid composition and concentration

Next, we evaluated whether the observed PD0325901-driven changes in gene and protein expression led to physiological effects on bile acid metabolism. While there was no significant difference in bile flow, the total biliary bile acid secretion into the bile was increased by on average 50 μmol/24 hr/100 g body weight in the PD0325901-treated mice, but this did not reach statistical significance (Fig. 4A, B, Table S1). To provide insight in the pathways involved in bile acid synthesis and metabolism, we measured the various bile acids (both taurine-conjugated and unconjugated) in bile and plasma. PD0325901 treatment altered the biliary bile acid composition, with an increased abundance of the primary bile acid cholic acid (CA) and taurine-conjugated CA (T-CA) and of the secondary bile acid taurodeoxycholic acid (T-DCA) (Fig. 4C, Tables S1, S2, S3), indicating increased activity of the classical pathway for bile acid synthesis. Furthermore, the abundance of β-muricholic acid (βMCA) and its conjugated form T-βMCA were significantly decreased in the bile (Fig. 4C, Tables S2 and S3). These differences resulted in an increased heuman index for hydrophobicity of the biliary bile acids in the PD0325901-treated group (Fig. 4D), indicating a more toxic bile acid composition. Total plasma bile acid levels were not affected (Fig. 4E), and the plasma bile acid composition remained largely unaltered except for an increased

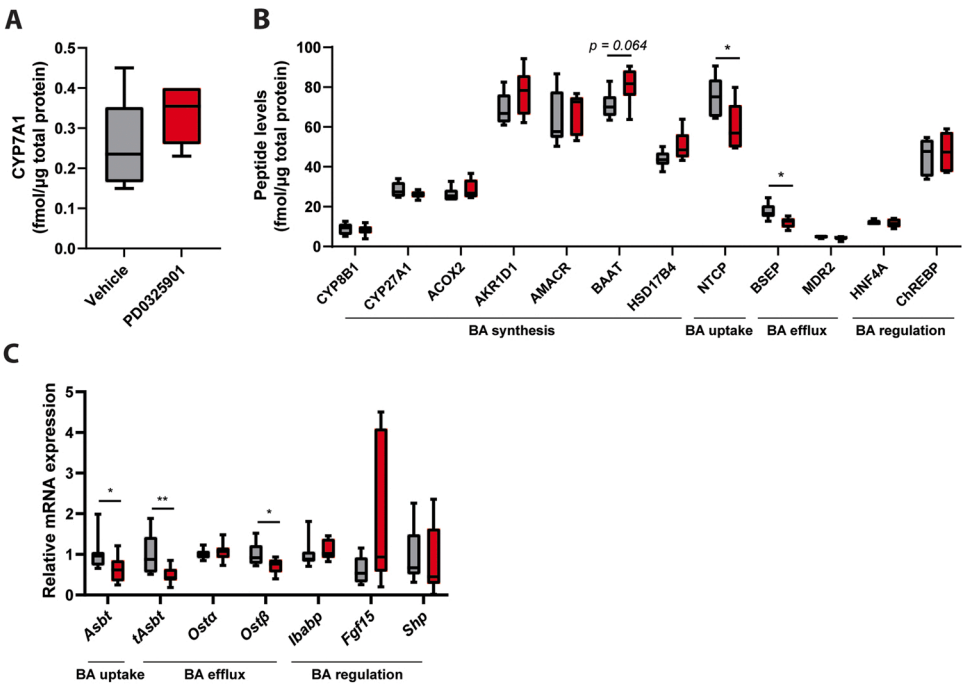

Fig. 3. Changes in genes and proteins involved in bile acid metabolism after PD0325901 or vehicle treatment. (A) Peptide levels of hepatic CYP7A1 using targeted proteomics (n = 6) and (B) peptide levels of other proteins involved in bile acid metabolism using targeted proteomics (n = 6). (C) Relative mRNA levels of genes involved in BA uptake, efflux, and regulation in the ileum of PD0325901-treated mice versus vehicle-treated mice, normalized to house-keeping gene *36b4* (n = 9). Data shown as box and whisker with mean ± min, max with * indicating $p < 0.05$, * * $p < 0.01$, * ** $p < 0.001$, and * *** * $p < 0.0001$.

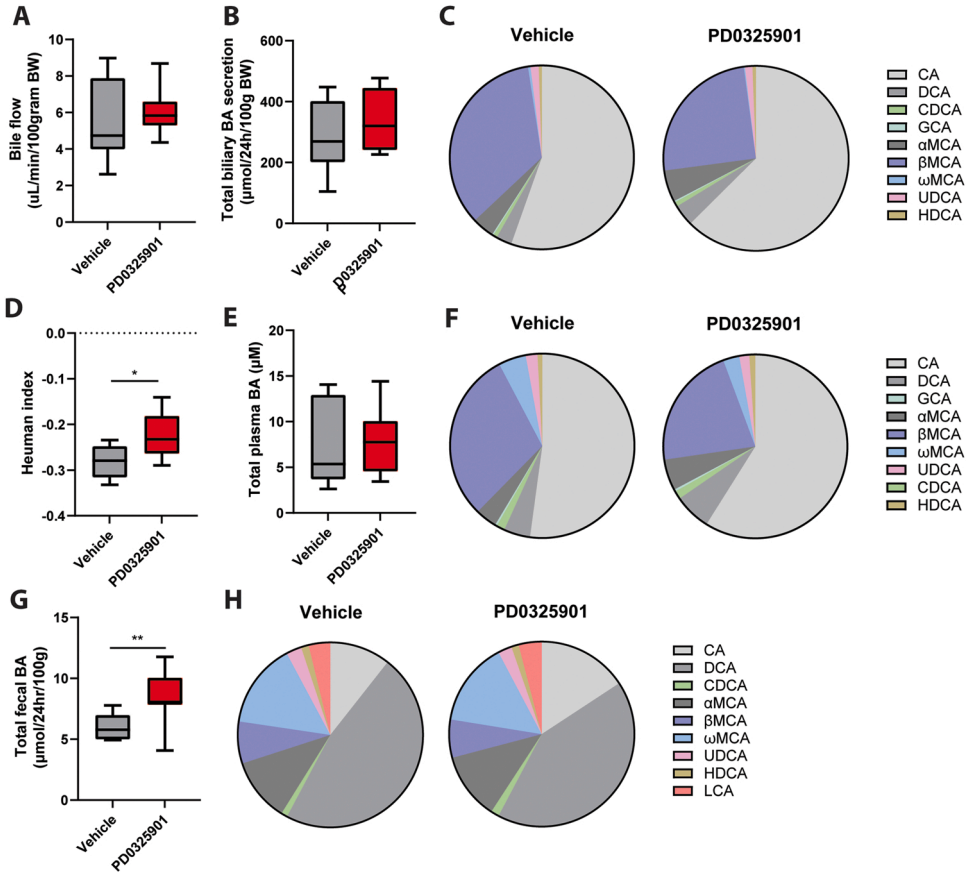

Fig. 4. Physiological and metabolic consequences due to PD0325901 treatment. (A) Bile flow, (B) total biliary bile acid secretion and (C) composition, and (D) heuman index after PD0325901 treatment or vehicle (n = 9). (E) Total plasma bile acids and (F) composition, and (G) total fecal bile acids and (H) composition after treatment with PD0325901 or vehicle (n = 9). Data shown as box and whisker with mean ± min, max with * indicating $p < 0.05$, * * $p < 0.01$.

abundance in T-αMCA and hepatotoxic T-DCA (Fig. 4F, Table S4, S5). Finally, to determine the rate of hepatic bile acid synthesis we measured fecal bile acid loss, which under steady state conditions is equal to synthesis by the liver. PD0325901-treated mice presented with a significantly increased total fecal bile acid excretion, mainly due to increased levels of CA (Fig. 4G, H, Table S6, S7, S8). Taken together, in steady state conditions, MEK inhibition increased fecal bile acid excretion, which indicates increased hepatic bile acid synthesis.

3.5. MEK inhibition induces markers of early liver toxicity

Elevated bile acid levels, especially of T-DCA, are toxic to cells. Therefore we investigated the effect of short-term PD0325901 treatment on hepatotoxicity or other adverse effects. Short-term PD0325901 treatment did not affect body weight, food intake, liver weight, or liver-to-body weight ratio compared to vehicle-treated mice (Fig. S3A-D). Next, we evaluated gene biomarkers of early liver toxicity involved in metabolism and detoxification, which have been shown to predict potential liver toxicity [24]. Gene biomarkers carnintine-O-acetyltransferase (Crat), triokinase/FMN cyclase (Tkfc), and carbonic anhydrase 3 (Car3) were all increased in livers of PD0325901-treated mice (Fig. S3I), indicating early hepatotoxicity upon PD0325901 treatment. However, there was no difference in the plasma markers of liver damage alanine transaminase (ALT) and plasma aspartate transaminase (AST) levels or AST/ALT ratio (Fig. S3E-F). In line, the expression of genes related to inflammation in the liver was also not affected by PD0325901 treatment (Fig. S3H). Plasma citrulline level, a marker of intestinal damage [25], was also not changed upon PD treatment (Fig. S3G). In conclusion, short-term PD0325901 treatment led to changes in predictive biomarkers of early liver toxicity, but this was not accompanied by apparent liver or intestinal damage.

3.6. MEK inhibitors increase CYP7A1 expression in human hepatocyte cell lines

Next, we evaluated if the regulation of *CYP7A1 and SHP* by MEK1/2 is conserved in humans by testing the effect of PD0325901 on three different human hepatocyte cell lines, HepG2, Hep3B, and IHH. A significant increase in *CYP7A1* (Fig. 5A) and a decrease in *SHP* were observed in all three cell lines (Fig. 5B). The effect of ERK inhibition on these and other genes involved in bile acid homeostasis was studied in more detail in IHH cells, a cell line derived from a healthy liver and immortalized by transfection with an SV40 large T antigen-expressing plasmid Schippers et al. [22]. The effects on *CYP7A1* and *SHP* could already be observed 30 min after PD0325901 treatment, and a dose-response experiment revealed that a concentration of 1 nM PD0325901 was enough to affect phosphorylation of ERK and the expression of *CYP7A1* and *SHP* (Fig. 5C, D). Similarly, the effect of PD0325901 that was observed on *ASBT* and *OSTα* in the mouse ileum was tested in differentiated Caco-2 cells, a human intestinal-like enterocyte model. Treatment with PD0325901 decreased phosphorylation of ERK, and in line with what we observed in mice, PD0325901 treatment decreased the expression of *ASBT* and *OSTα* (Fig. S4). However, while PD0325901 treatment did not affect *Shp* expression *in vivo*, it did decrease *SHP* expression in differentiated Caco-2 cells (Fig. S4).

Lastly, we tested the specificity of PD0325901 treatment by exploring the effect of several other FDA-approved BRAF (vemurafenib and dabrafenib) and MEK (selumetinib, trametinib, and PD0325901) inhibitors on *CYP7A1* and *SHP* gene expression in human hepatocyte cell lines. Treatment of human hepatocytes with all tested BRAF and MEK inhibitors, except for vemurafenib, resulted in a marked increase in *CYP7A1* and a decrease in *SHP* gene expression levels (Fig. 5E, F). In contrast, inhibition of upstream RTKs using various RTK inhibitors did not result in clear changes in the expression of *CYP7A1* and *SHP* in IHH and HepG2 cells (Fig. S5). Therefore, dysregulation of *CYP7A1* and *SHP* expression appears to be specific to pharmacological inhibition of the RAS-MAPK pathway.

4. Discussion

In the current study, we characterized the effect of pharmacological RAS-MAPK inhibition on hepatic transcription and function. Treatment of healthy C57BL/6 J mice with the MEK inhibitor PD0325901 affected the expression of over 400 genes in the liver, including pronounced changes in genes involved in bile acid homeostasis. We identified *Cyp7a1* as the top differentially affected gene, and its induction was linked to increased bile acid synthesis and a more hydrophobic bile acid composition. These findings highlight the importance of the RAS-MAPK pathway in the feedback regulation of bile acid metabolism.

The liver is a key metabolic organ and the main site for drug metabolism. Although preclinical studies have shown that pharmacological inhibition of the RAS-MAPK pathway decreases ERK phosphorylation in the liver, the molecular and functional consequences remain largely unknown [26]. In our study, transcriptome analysis of PD0325901-treated livers revealed that pharmacological MEK inhibition affects the expression of genes involved in various of signaling pathways and cellular processes. However, the most notable change was that decreased hepatic RAS-MAPK signaling led to a dramatic increase in *Cyp7a1* expression, while the expression of the transcriptional repressor *Shp* was strongly reduced. SHP is an atypical nuclear receptor that does not bind DNA but instead regulates the expression of genes via interactions with other nuclear receptors such as FXR, LRH-1, LXR α, and HNF4α [27,28]. Bile acid metabolism is tightly regulated by FXR, which senses intracellular levels of bile acids and controls bile acid-induced transcriptional programs, including feedback regulation via SHP. Feedback regulation of bile acid synthesis is mediated by FXR-induced expression of SHP, which in turn represses LRH-1 activity, thereby inhibiting *CYP7A1* expression [29]. In the present study, *Fxr* expression was upregulated, probably as a compensatory response, while the expression of *Shp* was nearly absent. The absence of *Shp* expression suggests that interaction between SHP and LRH-1 cannot occur, and *Cyp7a1* can no longer be repressed by FXR. In line with the increased *Cyp7a1* expression, PD0325901 treatment also increased CYP7A1 protein levels, and this was associated with changes in bile acid synthesis and composition. Supporting this finding, we observed an increase in the fecal bile acid excretion, which indicates an increase in hepatic bile acid synthesis. These findings are reminiscent of other mouse models with increased CYP7A1 expression. First, transgenic *Cyp7a1* overexpression in mice increases in bile acid pool size [30,31]. Similar to our findings, the fecal bile acid content was elevated, and the bile acid composition shifted towards a more hydrophobic content [31]. Second, *Shp* knockout mice, in which the negative feedback regulation of bile acid synthesis was also impaired, are characterized by an increased bile acid pool size [32,33]. Third, *Erk1/2* double knockout mice are characterized by a dramatic increase in *Cyp7a1* gene expression levels, while *Shp* gene expression is decreased [34]. Similar to PD0325901 treatment, *Erk1/2* double knockout mice also displayed increased bile acid levels and changes in bile acid composition with an increase in CA, T-CA, and αMCA levels [34].

Next to *Cyp7a1* and *Shp*, other genes involved in bile acid metabolism were also affected by PD0325901 treatment. *Ntcp* and *Bsep* are the primary bile acid transporters in hepatocytes that mediate bile acid flux from the portal blood into the bile. We found a reduction in hepatic NTCP and BSEP protein levels upon PD0325901 treatment, similar to what is observed in cholestatic liver diseases [35]. While NTCP mRNA expression levels were upregulated upon MEK inhibition, NTCP protein levels were reduced. *Ntcp* expression is controlled by bile acid-activated FXR via induction of repressor SHP. Loss of its repression because of decreased SHP levels likely explains the upregulation of NTCP mRNA expression levels [36]. However, NTCP protein levels are tightly regulated by post-translational modifications, and NTCP protein levels can be reduced to protect hepatocytes from elevated bile acid levels,

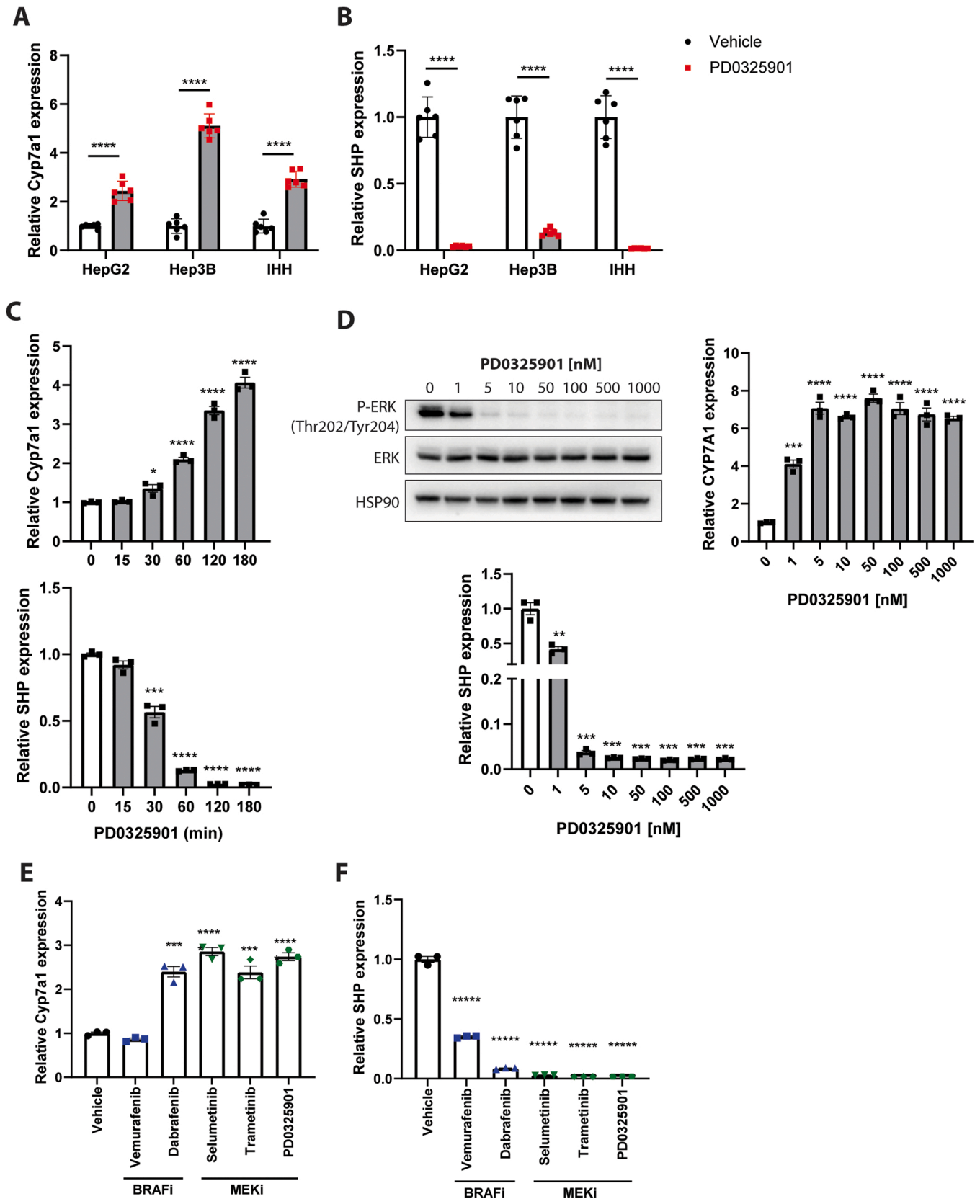

Fig. 5. Effect of PD0325901 in human hepatocyte cell lines. (A) Relative *CYP7A1* and (B) *SHP* expression after 6 h of treatment with 100 nM PD0326901 in IHH, HepG2, and Hep3B cell lines (n = 6). (C) Relative *CYP7A1* and *SHP* expression after 0, 15, 30, 60, 120 and 180 min of treatment with 100 nM PD0326901 in IHH cells (n = 3). (D) Western blot of phosphorylated ERK, total ERK and HSP90 and relative *CYP7A1* and *SHP* expression after treatment with 0, 1, 5, 10, 50, 100, 500 and 1000 nM PD0325901 in IHH cells (n = 3). (E) Relative Cyp7a1 and (F) SHP expression in IHH cells after 6 h of treatment with 100 nM Vemurafenib, Dabrafenib, Selumetinib, Trametinib, or PD0325901 (n = 3). Data shown as mean ± SEM with * indicating $p < 0.05$, * * $p < 0.01$, * ** $p < 0.001$, and * ** * $p < 0.0001$.

potentially explaining the reduced NTCP protein levels in our study [37]. In line, the absence of *Ntcp* in mice has been shown to result in reduced hepatic clearance of bile acids and elevated plasma bile acid levels [36,38]. Decreased BSEP levels are in concordance with previous studies, whereby TKI treatment of human hepatocytes also resulted in the inhibition of BSEP, an important mechanism of drug-induced liver injury caused by the hepatic accumulation of toxic bile acids [39–41]. The changes in bile acid metabolism due to PD0325901 treatment led to a higher hydrophobicity index of bile, mainly caused by an increase in CA and T-CA, which is generally associated with higher hepatic toxicity [42]. PD0325901-treated mice also presented differences in bile acid-related genes in the ileum, which are expected to contribute to the changes in whole-body bile acid metabolism. We found decreased mRNA expression of *Asbt*, which mediates the uptake of conjugated bile acids at the apical (luminal) side of enterocytes, and of *Ost-β*, which is present at the basolateral membrane mediating bile acid efflux from the enterocytes towards the circulation [23,43]. Lower levels of these transporters potentially explain the reduced intestinal reabsorption of bile acids [44].

While short-term PD0325901 treatment did not result in overt hepatotoxicity as measured by plasma ALT and AST levels, another study reported hepatotoxicity after chronic ERK deficiency [34]. Three weeks after the induction of *Erk1/2* double knockout by tamoxifen injection, mice present with liver injury, cholestasis, and increased plasma and hepatic bile acids. Five weeks after the knockout of *Erk1/2* by tamoxifen injection, mortality increased by 25 %. These observations indicate that long-term PD0325901 treatment will likely result in more substantial toxicity. In a clinical setting, changes in CYP7A1 enzyme activity and bile acid synthesis in patients could be monitored by measuring plasma 7alpha-hydroxy-4-cholesten-3-one (C4) [45–47]. In addition, plasma levels of FGF19 could be used as a biomarker of toxicity, as its levels are inversely correlated with plasma C4 levels and bile acid synthesis [48,49]. Although more clinical research is needed, we suggest that plasma C4 and FGF19 levels during TKI treatment in patients may serve as biomarkers to assess the early stages of bile acid-induced hepatotoxicity.

We found that the regulation of *Cyp7a1* and *Shp* by MEK1/2 was conserved in various human liver cells. In addition, we demonstrated that the regulation of *Cyp7a1* and *Shp* was not specific for PD0325901 but also occurred after exposure of cells to other FDA-approved BRAF and MEK inhibitors. In line with these observations, Saran et al. recently reported hepatotoxicity in response to various TKIs. They showed that pharmacological use of dasatinib, pazopanib, and sorafenib - inhibitors targeting multiple tyrosine kinases - elevated AST/ALT levels in 21–50 % of patients and increased CYP7A1 expression in human hepatocytes [39]. In our study, we tested the effect of additional TKIs on SHP and CYP7A1 gene expression. However, we found that the expression of these genes was mainly affected by inhibitors targeting MEK and BRAF, and to a much lesser extent by drugs targeting upstream receptor tyrosine kinases. These observations indicate that disruption of bile acid metabolism is less common to TKI inhibition but specific to the RAS-MAPK pathway.

Understanding the adverse effects of MEK inhibitors is also becoming increasingly relevant in combination therapies. Combined BRAF and MEK inhibitor therapies are now often used to overcome resistance mechanisms in cancers with BRAF mutations with promising results. For example, in phase 3 clinical trials, combination treatment with the BRAF inhibitor dabrafenib and the MEK inhibitor trametinib improved the overall response rate and survival in patients with metastatic melanoma or unresectable advanced melanoma with VRAF V600E or V600K mutations [50,51]. However, 26 % of patients in the combination therapy group discontinued the trial drug, while 38 % and 66 % of patients had an adverse event leading to dose reduction or interruption, respectively [51]. In addition, combining BRAF and MEK inhibitors with checkpoint inhibitor immunotherapies, such as inhibitors of programmed death 1 (PD-1), is an emerging therapy under investigation [52,53]. A phase 1/2 clinical trial assessed the safety and efficacy of the anti-PD-1 antibody pembrolizumab in combination with trametinib and dabrafenib in patients with advanced melanoma [54]. Although the triple-combination treatment increased the long-lasting antitumor responses, 73 % (11 out of 15 patients) experienced grade 3/4 adverse effects, with elevated liver function test levels and pyrexia as the most common effects, which could be resolved by interruption of dabrafenib and trametinib [54]. These studies indicate that liver toxicity is a critical problem in promising combination therapies.

Our study investigated the molecular mechanisms underlying MEK inhibitor-induced toxicity and identified changes in multiple regulators of bile acid metabolism, including transcriptional regulators, transporters, and cytochrome P450 enzymes. We propose that the observed changes in bile acid metabolism upon pharmacological inhibition of the RAS-MAPK pathway contribute to hepatotoxicity and gastrointestinal complications later in the treatment. As bile acids also act as hormones that activate multiple receptors (e.g., FXR, TGR5, VDR, and PXR), it is conceivable that MEK inhibitor-induced changes in bile acid homeostasis will also have pleiotropic effects on energy metabolism, inflammation, glucose homeostasis, drug metabolism and intestinal function (reviewed in Chávez-Talavera et al., 2017[55]). Future studies should uncover whether restoring of bile acid metabolism, e.g., by ursodeoxycholic acid (UDCA) or bile acid sequestrants, can prevent or delay hepatotoxicity in MEK combination treatments.

Significance statement

Small molecule inhibitors directed against the RAS-MAPK pathway are used to treat various malignancies, but side effects can result in treatment interruption, morbidity, and mortality. We show that short-term MEK inhibition deregulates the expression of genes involved in bile acid metabolism and consequently causes profound alterations in bile acid metabolism. Our work contributes to understanding the initial mechanisms by which RAS-MAPK inhibitors can cause gastrointestinal complications, hepatotoxicity, and related side effects.

CRediT authorship contribution statement

Cristy R.C. Verzijl: Conceptualization, Methodology, Writing – original draft, Formal analysis, Investigation, Visualization, Project administration. **Ivo P. van de Peppel:** Conceptualization, Methodology. **Roos E. Eilers:** Investigation. **Vincent W. Bloks:** Formal analysis, Software. **Justina C. Wolters:** Investigation, Formal analysis, Resources. **Martijn Koehorst:** Investigation, Formal analysis. **Niels J. Kloosterhuis:** Investigation, Resources. **Rick Havinga:** Investigation, Resources. **Mathilde Jalving:** Writing – review & editing. **Dicky Struik:** Conceptualization, Methodology, Writing – review & editing. **Johan W. Jonker:** Funding acquisition, Project administration, Conceptualization, Writing – original draft.

Conflict of interest statement

The authors have no conflicts of interest to declare.

Data availability

Data will be made available on request.

Acknowledgements

This study was supported by grants from The Netherlands Organization for Scientific Research (VICI grant 016.176.640 to JWJ) and the De Cock Stichting.

Appendix A. Supporting information

Supplementary data associated with this article can be found in the

online version at doi:10.1016/j.biopha.2023.114270.

References

[1] A. Ullrich, J. Schlessinger, Signal transduction by receptors with tyrosine kinase activity, Cell 61 (1990) 203–212, https://doi.org/10.1016/0092-8674(90)90801-k.

[2] M.A. Lemmon, J. Schlessinger, Cell signaling by receptor tyrosine kinases, Cell 141 (2010) 1117–1134, https://doi.org/10.1016/j.cell.2010.06.011.

[3] J.W. Ramos, The regulation of extracellular signal-regulated kinase (ERK) in mammalian cells, Int. J. Biochem. Cell Biol. 40 (2008) 2707–2719, https://doi.org/10.1016/j.biocel.2008.04.009.

[4] E.B. Ünal, F. Uhlitz, N. Blüthgen, A compendium of ERK targets, FEBS Lett. 591 (2017) 2607–2615, https://doi.org/10.1002/1873-3468.12740.

[5] M. Sinkala, P. Nkhoma, N. Mulder, D.P. Martin, Integrated molecular characterisation of the MAPK pathways in human cancers reveals pharmacologically vulnerable mutations and gene dependencies, Commun. Biol. 4 (2021) 9, https://doi.org/10.1038/s42003-020-01552-6.

[6] R.B. Corcoran, D. Dias-Santagata, K. Bergethon, et al., BRAF gene amplification can promote acquired resistance to MEK inhibitors in cancer cells harboring the BRAF V600E mutation, Sci. Signal 3 (2010) ra84, https://doi.org/10.1126/scisignal.2001148.

[7] V. Subbiah, C. Baik, J.M. Kirkwood, Clinical development of BRAF plus MEK inhibitor combinations, Trends Cancer 6 (2020) 797–810, https://doi.org/10.1016/j.trecan.2020.05.009.

[8] A.M. Gross, P.L. Wolters, E. Dombi, et al., Selumetinib in children with Inoperable plexiform neurofibromas, N. Engl. J. Med. 382 (2020) 1430–1442, https://doi.org/10.1056/NEJMoa1912735.

[9] S.J. Welsh, P.G. Corrie, Management of BRAF and MEK inhibitor toxicities in patients with metastatic melanoma, Ther. Adv. Med. Oncol. 7 (2015) 122–136, https://doi.org/10.1177/1758834014566428.

[10] L. Heinzerling, T.K. Eigentler, M. Fluck, et al., Tolerability of BRAF/MEK inhibitor combinations: adverse event evaluation and management, ESMO Open 4 (2019), e000491, https://doi.org/10.1136/esmoopen-2019-000491.

[11] L.J. Klesse, J.T. Jordan, H.B. Radtke, et al., The use of MEK inhibitors in neurofibromatosis type 1-associated tumors and management of toxicities, Oncologist 25 (2020) e1109–e1116, https://doi.org/10.1634/theoncologist.2020-0069.

[12] C. Glen, Y.Y. Tan, A. Waterston, et al., Mechanistic and clinical overview cardiovascular toxicity of BRAF and MEK inhibitors: JACC: cardiooncology state-of-the-art review, JACC CardioOncol. 4 (2022) 1–18, https://doi.org/10.1016/j.jaccao.2022.01.096.

[13] Q. Zhao, Z.E. Wu, B. Li, F. Li, Recent advances in metabolism and toxicity of tyrosine kinase inhibitors, Pharmacol. Ther. 237 (2022), 108256, https://doi.org/10.1016/j.pharmthera.2022.108256.

[14] F. Catalanotti, G. Reyes, V. Jesenberger, et al., A Mek1-Mek2 heterodimer determines the strength and duration of the Erk signal, Nat. Struct. Mol. Biol. 16 (2009) 294–303, https://doi.org/10.1038/nsmb.1564.

[15] B.D. Weiss, P.L. Wolters, S.R. Plotkin, et al., NF106: a Neurofibromatosis Clinical Trials Consortium Phase II Trial of the MEK inhibitor Mirdametinib (PD-0325901) in adolescents and adults with NF1-related plexiform neurofibromas, J. Clin. Oncol. J. Am. Soc. Clin. Oncol. 39 (2021) 797–806, https://doi.org/10.1200/JCO.20.02220.

[16] J. Desai, H. Gan, C. Barrow, et al., Phase I, open-label, dose-escalation/dose-expansion study of Lifirafenib (BGB-283), an RAF family kinase inhibitor, in patients with solid tumors, J. Clin. Oncol. J. Am. Soc. Clin. Oncol. 38 (2020) 2140–2150, https://doi.org/10.1200/JCO.19.02654.

[17] X. Yuan, Z. Tang, R. Du, et al., RAF dimer inhibition enhances the antitumor activity of MEK inhibitors in K-RAS mutant tumors, Mol. Oncol. 14 (2020) 1833–1849, https://doi.org/10.1002/1878-0261.12698.

[18] F. Kuipers, J.M. van Ree, M.H. Hofker, et al., Altered lipid metabolism in apolipoprotein E-deficient mice does not affect cholesterol balance across the liver, Hepatology 24 (1996) 241–247, https://doi.org/10.1002/hep.510240138.

[19] Oliveros J.C. , 2015. Venny. An interactive tool for comparing lists with Venn's diagrams, in: Venny 2.1.

[20] A. Fedoseienko, M. Wijers, J.C. Wolters, et al., The COMMD family regulates plasma LDL levels and attenuates atherosclerosis through stabilizing the CCC complex in endosomal LDLR trafficking, Circ. Res. 122 (2018) 1648–1660, https://doi.org/10.1161/CIRCRESAHA.117.312004.

[21] J.F. de Boer, E. Verkade, N.L. Mulder, et al., A human-like bile acid pool induced by deletion of hepatic Cyp2c70 modulates effects of FXR activation in mice, J. Lipid Res. 61 (2020) 291–305, https://doi.org/10.1194/jlr.RA119000243.

[22] I.J. Schippers, H. Moshage, H. Roelofsen, et al., Immortalized human hepatocytes as a tool for the study of hepatocytic (de-)differentiation, Cell Biol. Toxicol. 13 (1997) 375–386, https://doi.org/10.1023/a:1007404028681.

[23] B. Hagenbuch, P. Dawson, The sodium bile salt cotransport family SLC10, Pflug. Arch. 447 (2004) 566–570, https://doi.org/10.1007/s00424-003-1130-z.

[24] B.P. Smith, L.S. Auvil, M. Welge, et al., Identification of early liver toxicity gene biomarkers using comparative supervised machine learning, Sci. Rep. 10 (2020) 19128, https://doi.org/10.1038/s41598-020-76129-8.

[25] K.C. Fragkos, A. Forbes, Citrulline as a marker of intestinal function and absorption in clinical settings: a systematic review and meta-analysis. United Eur, Gastroenterol. J. 6 (2018) 181–191, https://doi.org/10.1177/2050640617737632.

[26] A.P. Brown, T.C.G. Carlson, C.-M. Loi, M.J. Graziano, Pharmacodynamic and toxicokinetic evaluation of the novel MEK inhibitor, PD0325901, in the rat following oral and intravenous administration, Cancer Chemother. Pharmacol. 59 (2007) 671–679, https://doi.org/10.1007/s00280-006-0323-5.

[27] Y. Zhang, C.H. Hagedorn, L. Wang, Role of nuclear receptor SHP in metabolism and cancer, Biochim. Biophys. Acta 1812 (2011) 893–908, https://doi.org/10.1016/j.bbadis.2010.10.006.

[28] Y.-S. Lee, D. Chanda, J. Sim, et al., Structure and function of the atypical orphan nuclear receptor small heterodimer partner, Int. Rev. Cytol. 261 (2007) 117–158, https://doi.org/10.1016/S0074-7696(07)61003-1.

[29] B. Goodwin, S.A. Jones, R.R. Price, et al., A regulatory cascade of the nuclear receptors FXR, SHP-1, and LRH-1 represses bile acid biosynthesis, Mol. Cell 6 (2000) 517–526, https://doi.org/10.1016/s1097-2765(00)00051-4.

[30] T. Li, E. Owsley, M. Matozel, et al., Transgenic expression of cholesterol 7alpha-hydroxylase in the liver prevents high-fat diet-induced obesity and insulin resistance in mice, Hepatology 52 (2010) 678–690, https://doi.org/10.1002/hep.23721.

[31] T. Li, M. Matozel, S. Boehme, et al., Overexpression of cholesterol 7α-hydroxylase promotes hepatic bile acid synthesis and secretion and maintains cholesterol homeostasis, Hepatology 53 (2011) 996–1006, https://doi.org/10.1002/hep.24107.

[32] L. Wang, Y.-K. Lee, D. Bundman, et al., Redundant pathways for negative feedback regulation of bile acid production, Dev. Cell 2 (2002) 721–731, https://doi.org/10.1016/s1534-5807(02)00187-9.

[33] T.A. Kerr, S. Saeki, M. Schneider, et al., Loss of nuclear receptor SHP impairs but does not eliminate negative feedback regulation of bile acid synthesis, Dev. Cell 2 (2002) 713–720, https://doi.org/10.1016/s1534-5807(02)00154-5.

[34] F. Cingolani, Y. Liu, Y. Shen, et al., Redundant functions of ERK1 and ERK2 maintain mouse liver homeostasis through down-regulation of bile acid synthesis, Hepatol. Commun. 6 (2022) 980–994, https://doi.org/10.1002/hep4.1867.

[35] G. Zollner, P. Fickert, R. Zenz, et al., Hepatobiliary transporter expression in percutaneous liver biopsies of patients with cholestatic liver diseases, Hepatology 33 (2001) 633–646, https://doi.org/10.1053/jhep.2001.22646.

[36] L.A. Denson, E. Sturm, W. Echevarria, et al., The orphan nuclear receptor, shp, mediates bile acid-induced inhibition of the rat bile acid transporter, ntcp, Gastroenterology 121 (2001) 140–147, https://doi.org/10.1053/gast.2001.25503.

[37] Y. Li, J. Zhou, T. Li, Regulation of the HBV entry receptor NTCP and its potential in hepatitis B treatment, Front. Mol. Biosci. 9 (2022), 879817, https://doi.org/10.3389/fmolb.2022.879817.

[38] J.M. Donkers, S. Kooijman, D. Slijepcevic, et al., NTCP deficiency in mice protects against obesity and hepatosteatosis, JCI Insight (2019) 5, https://doi.org/10.1172/jci.insight.127197.

[39] C. Saran, L. Sundqvist, H. Ho, et al., Novel bile acid-dependent mechanisms of hepatotoxicity associated with tyrosine kinase inhibitors, J. Pharmacol. Exp. Ther. 380 (2022) 114–125, https://doi.org/10.1124/jpet.121.000828.

[40] J.G. Kenna, K.S. Taskar, C. Battista, et al., Can bile salt export pump inhibition testing in drug discovery and development reduce liver injury risk? An international transporter consortium perspective, Clin. Pharmacol. Ther. 104 (2018) 916–932, https://doi.org/10.1002/cpt.1222.

[41] J.P. Jackson, K.M. Freeman St., R.L. Claire, et al., Cholestatic drug induced liver injury: a function of bile salt export pump inhibition and Farnesoid X receptor antagonism, Appl. Vitr Toxicol. 4 (2018) 265–279, https://doi.org/10.1089/aivt.2018.0011.

[42] P. Song, Y. Zhang, C.D. Klaassen, Dose-response of five bile acids on serum and liver bile Acid concentrations and hepatotoxicty in mice, Toxicol. Sci. 123 (2011) 359–367, https://doi.org/10.1093/toxsci/kfr177.

[43] C.J. Soroka, N. Ballatori, J.L. Boyer, Organic solute transporter, OSTalpha-OSTbeta: its role in bile acid transport and cholestasis, Semin. Liver Dis. 30 (2010) 178–185, https://doi.org/10.1055/s-0030-1253226.

[44] P.A. Dawson, J. Haywood, A.L. Craddock, et al., Targeted deletion of the ileal bile acid transporter eliminates enterohepatic cycling of bile acids in mice, J. Biol. Chem. 278 (2003) 33920–33927, https://doi.org/10.1074/jbc.M306370200.

[45] C. Gälman, I. Arvidsson, B. Angelin, M. Rudling, Monitoring hepatic cholesterol 7alpha-hydroxylase activity by assay of the stable bile acid intermediate 7alpha-hydroxy-4-cholesten-3-one in peripheral blood, J. Lipid Res. 44 (2003) 859–866, https://doi.org/10.1194/jlr.D200043-JLR200.

[46] G. Sauter, F. Berr, U. Beuers, et al., Serum concentrations of 7alpha-hydroxy-4-cholesten-3-one reflect bile acid synthesis in humans, Hepatology 24 (1996) 123–126, https://doi.org/10.1053/jhep.1996.v24.pm0008707250.

[47] M. Axelson, A. Aly, J. Sjövall, Levels of 7 alpha-hydroxy-4-cholesten-3-one in plasma reflect rates of bile acid synthesis in man, FEBS Lett. 239 (1988) 324–328, https://doi.org/10.1016/0014-5793(88)80944-x.

[48] W.-Y. Liu, D.-M. Xie, G.-Q. Zhu, et al., Targeting fibroblast growth factor 19 in liver disease: a potential biomarker and therapeutic target, Expert Opin. Ther. Targets 19 (2015) 675–685, https://doi.org/10.1517/14728222.2014.997711.

[49] Z. Li, B. Lin, G. Lin, et al., Circulating FGF19 closely correlates with bile acid synthesis and cholestasis in patients with primary biliary cirrhosis, PLoS One 12 (2017), e0178580, https://doi.org/10.1371/journal.pone.0178580.

[50] G.V. Long, D. Stroyakovskiy, H. Gogas, et al., Combined BRAF and MEK inhibition versus BRAF inhibition alone in melanoma, N. Engl. J. Med. 371 (2014) 1877–1888, https://doi.org/10.1056/NEJMoa1406037.

[51] G.V. Long, A. Hauschild, M. Santinami, et al., Adjuvant dabrafenib plus Trametinib in stage III BRAF-mutated melanoma, N. Engl. J. Med. 377 (2017) 1813–1823, https://doi.org/10.1056/NEJMoa1708539.

[52] R. Offringa, L. Kötzner, B. Huck, K. Urbahns, The expanding role for small molecules in immuno-oncology, Nat. Rev. Drug Discov. (2022), https://doi.org/10.1038/s41573-022-00538-9.
[53] T. Rager, A. Eckburg, M. Patel, et al., Treatment of metastatic melanoma with a combination of immunotherapies and molecularly targeted therapies, Cancers) (2022) 14, https://doi.org/10.3390/cancers14153779.
[54] A. Ribas, D. Lawrence, V. Atkinson, et al., Combined BRAF and MEK inhibition with PD-1 blockade immunotherapy in BRAF-mutant melanoma, Nat. Med. 25 (2019) 936–940, https://doi.org/10.1038/s41591-019-0476-5.
[55] O. Chávez-Talavera, A. Tailleux, P. Lefebvre, B. Staels, Bile acid control of metabolism and inflammation in obesity, type 2 diabetes, dyslipidemia, and nonalcoholic fatty liver disease, Gastroenterology 152 (2017) 1679–1694.e3, https://doi.org/10.1053/j.gastro.2017.01.055.
[56] D.W. Huang, B.T. Sherman, R.A. Lempicki, Systematic and integrative analysis of large gene lists using DAVID bioinformatics resources, Nat. Protoc. 4 (2009) 44–57, https://doi.org/10.1038/nprot.2008.211.
[57] B.T. Sherman, M. Hao, J. Qiu, et al., DAVID: a web server for functional enrichment analysis and functional annotation of gene lists (2021 update), Nucleic Acids Res. (2022), https://doi.org/10.1093/nar/gkac194.